

## Large Enhancement of the Sub-barrier Fusion Probability for a Halo Nucleus

M. Trotta,<sup>1,2</sup> J.L. Sida,<sup>1</sup> N. Alamanos,<sup>1</sup> A. Andreyev,<sup>3</sup> F. Auger,<sup>1</sup> D.L. Balabanski,<sup>3</sup> C. Borcea,<sup>4</sup> N. Coulier,<sup>3</sup> A. Drouart,<sup>1</sup> D.J.C. Durand,<sup>1</sup> G. Georgiev,<sup>3</sup> A. Gillibert,<sup>1</sup> J.D. Hinfefeld,<sup>5,6</sup> M. Huyse,<sup>3</sup> C. Jouanne,<sup>1</sup> V. Lapoux,<sup>1</sup> A. Lépine,<sup>7</sup> A. Lumbroso,<sup>1</sup> F. Marie,<sup>1</sup> A. Musumarra,<sup>5</sup> G. Neyens,<sup>3</sup> S. Ottini,<sup>1</sup> R. Raabe,<sup>3</sup> S. Ternier,<sup>3</sup> P. Van Duppen,<sup>3</sup> K. Vyvey,<sup>3</sup> C. Volant,<sup>1</sup> and R. Wolski<sup>8</sup>

<sup>1</sup>DSM/DAPNIA, CEA SACLAY, 91191 Gif-sur-Yvette, France

<sup>2</sup>University of Napoli and INFN Sezione di Napoli, Napoli, Italy

<sup>3</sup>IKS, University of Leuven, Leuven, Belgium

<sup>4</sup>IPNE, Bucharest-Magurele, P.O. Box MG6, Romania

<sup>5</sup>Centre de Recherche du Cyclotron, UCL Louvain-la-Neuve, Belgium

<sup>6</sup>Physics Department, Indiana University, South Bend, 46615 Indiana

<sup>7</sup>IFU, Sao Paulo, CP 20156, Sao Paulo, Brazil

<sup>8</sup>Institute of Nuclear Physics, Cracow, Poland

(Received 27 September 1999)

The fusion-fission cross sections of the  ${}^4\text{He} + {}^{238}\text{U}$  and  ${}^6\text{He} + {}^{238}\text{U}$  systems have been measured, at Louvain-la-Neuve, for energies around and below the Coulomb barrier, using an array of Si detectors surrounding a  $\text{UF}_4$  target. The data taken with  ${}^4\text{He}$  are in good agreement with previous data and with the coupled channel fusion calculation performed with ECIS. The  ${}^6\text{He}$  data show a regular trend with a large enhancement below the barrier which is attributed to the halo structure of the  ${}^6\text{He}$  nucleus.

PACS numbers: 21.10.Gv, 25.60.-t, 25.70.Jj, 27.20.+n

The sub-barrier fusion of two nuclei is classically forbidden, and can be achieved only by quantum tunneling. The influence of the nuclear deformation on the fusion probability has been studied for stable nuclei, and a high sensitivity to the nuclear structure has been observed [1]. The major remaining questions concern the influence of other processes such as transfer or breakup reactions, as well as the effect of unusual structures of nuclei, such as neutron skins or halos [2]. Theoretical calculations agree that the large spatial extension of halo nuclei and the coupling with eventual low lying resonant states would increase the fusion cross section [3–6]. However, they strongly disagree on the role of the breakup effect on the fusion probability. This reaction could be seen as another doorway state to fusion [5] that would lead to an extra enhancement of the cross section or, on the other hand, as a loss of flux for fusion [4,6] that would decrease the cross section.

These calculations have been performed for the  ${}^{11}\text{Li} + {}^{208}\text{Pb}$  and  ${}^{11}\text{Li} + {}^{238}\text{U}$  systems. An experimental study of these systems is currently difficult due to the weak intensities that can be obtained for  ${}^{11}\text{Li}$  radioactive beams. Measurements of sub-barrier fusion for other halo nuclei have started, in 1991, at GANIL (France) with the fusion-fission cross section study of  ${}^{11}\text{Be} + {}^{238}\text{U}$ . However, these results did not lead to firm conclusions due to the lack of statistics [7]. At NSCL (MSU in the USA), the fusion-fission of the stable  ${}^{32}\text{S}$  and the unstable  ${}^{38}\text{S}$  nuclei on a  ${}^{181}\text{Ta}$  target have been measured [8]. An increase of the cross section for  ${}^{38}\text{S}$  has been observed that could be explained by a simple shift in the barrier height. Similar results have been obtained on the proton-rich side for the fusion-fission of  ${}^{17}\text{F} + \text{Pb}$  [9]. Other groups used

the identification of the residual nuclei via their alpha emission to reconstruct the fusion probability. At RIKEN (Japan), the  ${}^{11}\text{Be} + {}^{209}\text{Bi}$  system has been studied and the authors conclude that “*the contribution of the break-up process to the fusion is modest*” [10] and that “*the two cross-sections (for  ${}^9\text{Be} + {}^{209}\text{Bi}$  and  ${}^{11}\text{Be} + {}^{209}\text{Bi}$  are rather similar*” [11]. Studies have also been done with the  ${}^6\text{He}$  Borromean neutron-rich nucleus that presents a large spatial neutron distribution [12,13] with an inner core of  ${}^4\text{He}$ . It will be called a halo nucleus throughout this paper even if the question is still open. The  ${}^6\text{He} + {}^{209}\text{Bi}$  system [14,15] has been measured at Notre Dame (U.S.A.) with a similar technique and “*a large enhancement of sub-barrier fusion is observed*” [15]. Therefore both theoretical and experimental information gave contradictory answers to this problem.

In this Letter we report on a measurement of absolute fusion-fission cross sections of the  ${}^{4,6}\text{He} + {}^{238}\text{U}$  systems at energies above and below the barrier. The structure of  ${}^6\text{He}$  leads to an enhancement of the fusion probability at sub-barrier energies with respect to the fusion induced by the stable  ${}^4\text{He}$  isotope or by the  ${}^6\text{Li}$  nucleus which has the same mass number as  ${}^6\text{He}$  and a very close radius.

At energies around the barrier, the Pu compound nucleus formed by fusion of the  ${}^{4,6}\text{He} + {}^{238}\text{U}$  systems has an excitation energy much higher than the fission barrier and decays by fission. Fission could also be triggered by an inelastic or a transfer reaction. In such cases, the fission will be accompanied by a residue of the projectile that could be detected in coincidence in a high efficiency setup and thus disentangled from a fusion-fission event.

The experiment was performed at Cyclone, the Radioactive Nuclear Beam facility of Louvain-la-Neuve (Belgium) [16]. The setup provides an energy measurement of particles with a large angular coverage. It is composed of two open cubes placed on each side of the target. The faces perpendicular to the beam have been removed to let the beam pass through. Each face is composed of a set of four silicon detectors with a surface of  $50 \times 50 \text{ mm}^2$  and a thickness of  $500 \text{ }\mu\text{m}$ . The mechanics and the electronics have been constructed with special care in order to reduce the dead zones. The angular coverage is of the order of 70% of  $4\pi$ . The measurement of two particles emitted back to back has been optimized by a symmetric design with respect to the target point. The high granularity of 32 detectors allows the measurement of three particles in coincidence with a low pileup probability. Coincidence of two detectors provides the major trigger for the acquisition. Some single events were also recorded to measure elastic scattering, but their trigger rate was downscaled by a factor of  $10^5$ .

The detection efficiency was measured for each detector using a calibrated thin californium source which allows the detection of the two fission fragments. The global efficiency, defined as the ratio of the detected fission fragments to the number of fissions emitted from the source, is extracted using the same analysis as in the experiment itself. The energy calibrations were done with a three-peak alpha source, the californium source, and a pulser.

Two primary beam energies were used for the  $^4\text{He}$  isotope and four for the  $^6\text{He}$  isotope (Table I). The  $^4\text{He}$  energies were chosen to complement previous experiments [17,18]. The  $^6\text{He}$  energies covered the region around the barrier. Intermediate energies have been obtained using Mylar absorbers of thicknesses 25 and  $50 \text{ }\mu\text{m}$ . The angular and energy straggling introduced by these absorbers have been measured previously with position sensitive silicon detectors [19]. The beams were pure and their in-

intensities varied from  $2 \times 10^5$  particles per second (pps) to  $5 \times 10^6$  pps for  $^6\text{He}$  (Table I).

The beam intensity was measured during the experiment by a NE102 plastic scintillator placed at 0 deg for beam intensities less than  $7 \times 10^5$  pps. The pileup events and the activity in the monitor have been taken into account during all the runs via the time of flight measured with respect to the radio frequency of the cyclotron and the energy deposited in the plastic. For higher intensities, elastic scattering on the target was used. A silicon detector was placed at an angle around  $20^\circ$ . The silicon/plastic ratio was measured at low intensity and for each energy and absorber with a precision better than 3%. The intensity was then increased to the maximum value and monitored by the silicon detector. This provided a unique standard reference with the plastic.

The uranium targets were provided by the GSI laboratory [20]. They consist of  $\text{UF}_4$  deposited on a thin carbon foil of  $30 \text{ }\mu\text{g}/\text{cm}^2$  by thermal evaporation out of a tantalum crucible. They are fixed on an aluminum oval frame defining an area of  $8 \times 12 \text{ mm}^2$ . The target thickness was  $800 \text{ }\mu\text{g}/\text{cm}^2$  which is equivalent to a  $600 \text{ }\mu\text{g}/\text{cm}^2$  of pure U target. The uncertainty of the thickness is estimated to be 10% and the inhomogeneity of the target is 3%. The same target was used for the measurements with both He isotopes.

The energy spectrum from one detector is presented on the upper part of Fig. 1 for the measurement of  $^6\text{He} + ^{238}\text{U}$  at 25.3 MeV. The elastic scattering peak, the pulser peak, the pedestal, and  $\beta$  background at low energy are clearly seen. The fission fragments are the counts at the highest energies. Requiring that two detectors fire back to back and summing the statistics from the 32 detectors, the spectrum presented on the lower part of the figure is obtained for  $^6\text{He} + ^{238}\text{U}$  at 25.3 MeV (highest statistics) and for  $^6\text{He} + ^{238}\text{U}$  at 14.6 MeV (lowest statistics). A very weak number of events with three detectors fired has

TABLE I. Summary of the measurements for the different energies. The energies in bold correspond to direct beams from the cyclotron, while the other ones were obtained using the Mylar absorbers.

Beam	$E_{\text{c.m.}}$ (MeV)	I (pps)	Time	$N_{\text{fiss}}$	$\sigma_{\text{fiss}}$ (mb)	$\Delta\sigma_{\text{fiss}}^{\text{stat}}$ (mb)
$^4\text{He}$	<b>22.6</b>	$2.11 \times 10^8$	56 min	18 059	200.1	20.5
	21.6	$1.46 \times 10^8$	53 min	6074	93.9	9.5
	20.7	$9.95 \times 10^7$	51 min	1324	33.6	3.6
	<b>19.6</b>	$3.66 \times 10^8$	2h 25 min	1525	4.8	0.3
	18.5	$1.53 \times 10^8$	2h 44 min	194	0.87	0.08
	17.4	$1.38 \times 10^8$	5h 36 min	51	0.06	0.01
$^6\text{He}$	<b>28.7</b>	$1.72 \times 10^5$	1h 19 min	241	1381.0	99.1
	27.7	$1.71 \times 10^5$	2h 12 min	350	1480.1	84.0
	26.6	$1.31 \times 10^5$	3h 10 min	296	1140.7	71.4
	<b>25.3</b>	$5.78 \times 10^5$	3h 10 min	1134	1033.5	33.8
	24.2	$3.34 \times 10^5$	3h 6 min	570	794.2	36.0
	23.0	$1.61 \times 10^5$	4h 47 min	268	482.0	30.9
	<b>17.5</b>	$7.96 \times 10^5$	15h 7 min	301	37.3	2.2
	<b>14.6</b>	$5.29 \times 10^6$	16h 31 min	267	5.4	0.4

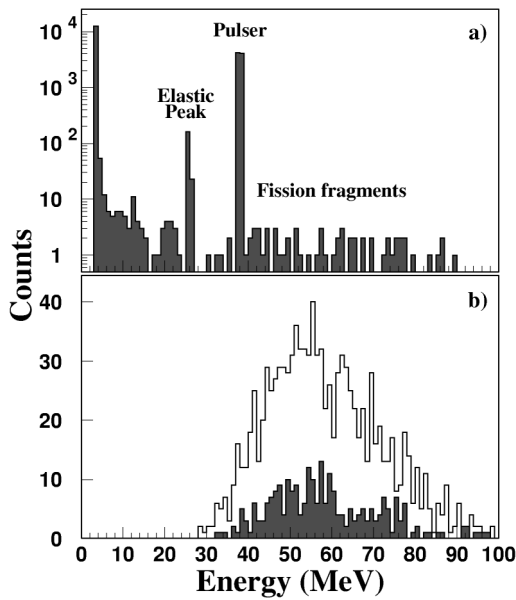


FIG. 1. Energy spectra obtained in the silicon detectors. (a) Raw spectrum for one detector for  ${}^6\text{He} + {}^{238}\text{U}$  at 25.3 MeV. The single (elastic scattering) events have been divided by  $10^5$ . (b) spectrum obtained asking the coincidence back to back for the set of 32 detectors for  ${}^6\text{He} + {}^{238}\text{U}$  at 25.3 MeV (highest statistics) and at 14.6 MeV (filled histogram).

been observed during all the measurements (less than 10%).

The main information concerning the data is presented in the Table I: center of mass energy of the beam at the center of the target, beam intensity, time of measurement, number of fissions detected, cross section, and statistical uncertainty. The statistical uncertainties are not directly correlated to the total number of fissions reported on the table since the cross sections have been determined on the basis of the number of fissions in each back-to-back pair of detectors and taking into account their measured efficiency.

The absolute fission cross sections are presented in Fig. 2 for  ${}^4\text{He} + {}^{238}\text{U}$  and  ${}^6\text{Li} + {}^{238}\text{U}$ . The full points have been extracted in this experiment. The uncertainties plotted in Fig. 2 are statistical only and are generally smaller than the symbol. The systematic uncertainties, 10% due to the target thickness and about 8% due to the efficiency of detection, could affect only the global normalization but not the relative cross sections since all the measurements have been performed under similar conditions. The results for  ${}^4\text{He} + {}^{238}\text{U}$  are in good agreement with previous measurements [17] (open square points), [18]. The  ${}^6\text{Li} + {}^{238}\text{U}$  fission cross sections (open circles) [21] are presented on the same figure but shifted in energy by the ratio of the charge of the projectiles. This allows one to compare the cross sections, taking into account the barrier change of the two systems. The  ${}^6\text{He}$  and  ${}^6\text{Li}$  have the same mass number and very close radii [13,22]. The difference in the trend of the two cross sections is due to the difference in the structure of these two nuclei.

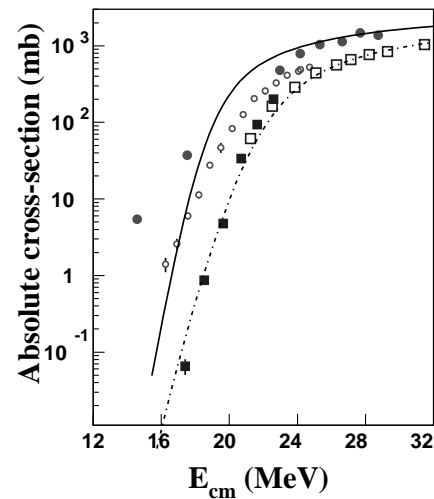


FIG. 2. Absolute fission cross section for  ${}^4\text{He} + {}^{238}\text{U}$  (full squares) and for  ${}^6\text{He} + {}^{238}\text{U}$  (full circles). The open squares are the results of [17]. The open circles are the fission cross sections for  ${}^6\text{Li} + {}^{238}\text{U}$  [21] shifted in energy (see text). The line (respectively, dotted line) corresponds to ECIS calculations for  ${}^6\text{He} + {}^{238}\text{U}$  (respectively,  ${}^4\text{He} + {}^{238}\text{U}$ ).

The two curves (solid line for  ${}^6\text{He}$  and dashed line for  ${}^4\text{He}$ ) plotted on the figure correspond to the ECIS [23] coupled channel fusion calculations. The potential has been calculated by the double-folding method [24] using the density-dependent nucleon-nucleon interaction called BDM3Y1 [25]. The densities of  ${}^4\text{He}$  and  ${}^{238}\text{U}$  are extracted from electron scattering measurement [22]. The density of  ${}^6\text{He}$  was obtained from shell model calculations [26]. The excited  $2^+$  state at 44.9 keV [ $B(E_2) = 12.3e^2b^2$  [27]],  $4^+$  at 148.4 keV,  $6^+$  at 307 keV, and  $8^+$  at 518 keV of  ${}^{238}\text{U}$  were coupled in the calculation. A Woods-Saxon form was chosen for the imaginary part of the potential with parameters simulating the incoming wave boundary condition. Calculations using different nucleon-nucleon interactions (M3Y, DDM3Y, ...) provide the same theoretical predictions.

The calculations are in good agreement with the measured cross sections for  ${}^4\text{He}$  and for  ${}^6\text{He}$  at energies above the barrier. Below the barrier, the fission cross section for the halo nucleus is much larger than the one expected from the fusion calculation. The ECIS calculations take explicitly into account the density of the colliding nuclei and the microscopic structure of  ${}^{238}\text{U}$ . Therefore, the large difference between the data and the calculated cross section is originating from the very peculiar role of the structure of  ${}^6\text{He}$  in the entrance of the fission process.

In order to quantify the difference between the cross sections, the data have been fitted with the Wong formula [28]. A good reproduction is obtained using a barrier height  $V_b = 21.3$  MeV, a radius of the barrier  $R_b = 10$  fm, and a curvature  $\hbar\omega = 3.6$  MeV for  ${}^4\text{He}$ , and  $V_b = 20.28$  MeV,  $R_b = 12.5$  fm, and  $\hbar\omega = 7.9$  MeV for  ${}^6\text{He}$  (inset of Fig. 3). The parameters extracted for the  ${}^6\text{He}$  nucleus are in good agreement with those of the potential

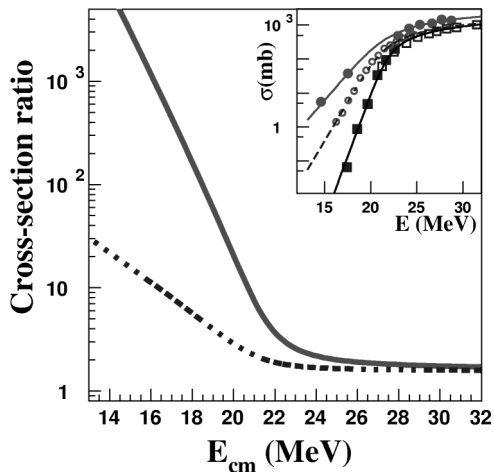


FIG. 3. Ratio of the cross sections:  ${}^6\text{He} + {}^{238}\text{U}$  over  ${}^4\text{He} + {}^{238}\text{U}$  (solid line) and  ${}^6\text{He} + {}^{238}\text{U}$  over  ${}^6\text{Li} + {}^{238}\text{U}$  (dashed line). The inset represents the cross sections with the curves resulting from the fit with the Wong formula.

calculated in the double folding method except for the curvature which was of 3.6 MeV in the folding calculation instead of 7.9 MeV from the result of the fit. This value corresponds to a much thinner one-dimensional barrier. Using this parametrization of the data, the ratio of the cross sections for the two isotopes has been extracted (full curve of Fig. 3). The same procedure has been applied for the ratio of the  ${}^6\text{He}$  cross sections over the shifted  ${}^6\text{Li}$  cross sections (dashed curve of Fig. 3). At energies above the barrier, the fusion cross section tends toward the reaction cross section, so the ratio of the curves tends to a constant. Below the barrier, the large enhancement is emphasized and reaches 3 orders of magnitude for the lowest energy, comparing to the measurement with  ${}^4\text{He}$ , and 1 order of magnitude comparing to the measurement with  ${}^6\text{Li}$ .

The contributions to fission from transfer reaction or inelastic scattering are weak since only a small number of events with three detectors fired were observed. The enhancement of the fusion probability for  ${}^6\text{He} + {}^{238}\text{U}$  under the barrier could not be explained by a simple shift of the barrier height as in [8] and is in contradiction with the results obtained with the  ${}^{11}\text{Be}$  nucleus [10]. This enhancement is even larger than the one calculated [3–5] for  ${}^{11}\text{Li}$  projectiles for equivalent  $E_{c.m.}/V_b$  values. It confirms, with a different technique, the enhancement observed in the three-neutron evaporation channel of the  ${}^6\text{He} + {}^{209}\text{Bi}$  system [15]. The very different curvature values obtained from the potential calculated by the double folding method (3.6 MeV) and extracted from the data by the fit with the Wong formula (7.9 MeV) are a signature of a very different fusion process for nuclei with low binding energies that develop halos or neutron skins. This is confirmed by the

ECIS calculations that did not take into account the peculiar structure of  ${}^6\text{He}$  and fail to reproduce the data below the barrier for this nucleus.

In summary, the effect of the halo on the fusion-fission probability was measured above and below the barrier for the systems  ${}^4,6\text{He} + {}^{238}\text{U}$ . The data lead us to conclude that at the barrier no hindrance due to the breakup of the nucleus is observed, and below the barrier there is a large enhancement of the fusion probability for the  ${}^6\text{He}$  nucleus with respect to the stable  ${}^4\text{He}$  nucleus.

We would like to thank the Louvain-la-Neuve cyclotron team for their constant help, the GSI laboratory, especially B. Lommel and P. Armbruster, for providing us uranium targets, and Y. Blumenfeld and D. Kusmirek for their careful reading of the script. This text represents research which was partly carried out under the Belgian programme of Interuniversity Poles of Attraction.

- [1] M. Beckerman, Rep. Prog. Phys. **51**, 1047 (1988).
- [2] I. Tanihata *et al.*, Phys. Rev. Lett. **55**, 2676 (1985).
- [3] N. Takigawa and H. Sagawa, Phys. Lett. B **265**, 23 (1991).
- [4] M. S. Hussein *et al.*, Phys. Rev. C **46**, 377 (1992); M. S. Hussein *et al.*, Phys. Rev. C **51**, 846 (1995).
- [5] C. H. Dasso and R. Donangelo, Phys. Lett. B **276**, 1 (1992); C. H. Dasso and A. Vitturi, Phys. Rev. C **50**, R12 (1994).
- [6] N. Takigawa, M. Kuratani, and H. Sagawa, Phys. Rev. C **47**, 2470 (1993).
- [7] V. Fekou-Youmbi *et al.*, Nucl. Instrum. Methods Phys. Res., Sect. A **437**, 490 (1999).
- [8] K. E. Zyromski *et al.*, Phys. Rev. C **55**, R562 (1997).
- [9] K. E. Rehm *et al.*, Phys. Rev. Lett. **81**, 3341 (1998).
- [10] A. Yoshida *et al.*, Phys. Lett. B **389**, 457 (1996).
- [11] C. Signorini *et al.*, Eur. Phys. J. A **2**, 227 (1998).
- [12] M. V. Zhukov *et al.*, Phys. Rep. **231**, 151 (1993).
- [13] G. D. Alkharov *et al.*, Phys. Rev. Lett. **78**, 2313 (1997).
- [14] P. A. DeYoung *et al.*, Phys. Rev. C **58**, 3442 (1998).
- [15] J. J. Kolata *et al.*, Phys. Rev. Lett. **81**, 4580 (1998).
- [16] M. Loiselet *et al.*, in *Proceedings of the 14th International Conference on Cyclotrons and Their Applications, Cape Town, South Africa, 1995* (World Scientific, Singapore, 1996).
- [17] V. E. Viola, Jr. and T. Sikkeland, Phys. Rev. **128**, 767 (1962).
- [18] H. Freiesleben and J. R. Huizenga, Nuc. Phys. **A224**, 503 (1974).
- [19] C. Jouanne *et al.*, Cyclone Annual Report (1997), p. 13.
- [20] B. Lommel, GSI Target Lab. (private communication).
- [21] H. Freiesleben *et al.*, Phys. Rev. C **12**, 43 (1975).
- [22] C. A. de Jager *et al.*, At. Data Nucl. Data Tables **14**, 479 (1974).
- [23] J. Raynal, Phys. Rev. C **23**, 2571 (1981).
- [24] G. R. Satchler and W. G. Love, Phys. Rep. **55**, 183 (1979).
- [25] D. T. Khoa *et al.*, Phys. Rev. C **56**, 954 (1997).
- [26] S. Karataglidis *et al.*, nucl-th/9811045; (private communication).
- [27] F. K. McGowan *et al.*, Phys. Rev. Lett. **27**, 1741 (1971).
- [28] C. Y. Wong, Phys. Rev. Lett. **12**, 766 (1973).